REMOTE SENSING APPLICATIONS IN FORESTRY

A report of research performed under the auspices of the

Forestry Remote Sensing Laboratory,
School of Forestry and Conservation
University of California
Berkeley, California

A Coordination Task Carried Out in Cooperation with
The Forest Service, U.S. Department of Agriculture

For

EARTH RESOURCES SURVEY PROGRAM
OFFICE OF SPACE SCIENCES AND APPLICATIONS
NATIONAL AERONAUTICS AND SPACE ADMINISTRATION

NASA order W-12,996

REMOTE SENSING APPLICATIONS IN FORESTRY

THE DEVELOPMENT OF AN EARTH RESOURCES INFORMATION SYSTEM USING AERIAL PHOTOGRAPHS AND DIGITAL COMPUTERS

by
Philip G. Langley
Jan Van Roessel
David A. Sharpnack
Robert M. Russell

Pacific Southwest Forest and Range Experiment Station
Forest Service, U. S. Department of Agriculture

Annual Progress Report 30 September, 1970

A report of research performed under the auspices of the

Forestry Remote Sensing Laboratory,
School of Forestry and Conservation
University of California
Berkeley, California
A Coordination Task Carried Out in Cooperation with
The Forest Service, U.S. Department of Agriculture

For

EARTH RESOURCES SURVEY PROGRAM
OFFICE OF SPACE SCIENCES AND APPLICATIONS
NATIONAL AERONAUTICS AND SPACE ADMINISTRATION

ABSTRACT

Work has continued toward fulfilling the three main objectives of this research effort. These are (1) to develop an operating earth resources information system oriented toward wildland applications, (2) to provide techniques for scanning and interpreting aerial photographs automatically to provide inputs to the information system, and (3) to develop sampling designs which optimally utilize the information system and supplementary remote sensor and ground data for resource inventory and analysis.

A systems analysis has been completed specifying the equipment and software packages needed to build the wildland information system. Programs have been written for data input while routines for storage and retrieval are under development.

We have tested several image matching procedures used in the automatic mapping of forest resources using digitized stereopairs of aerial photographs. Programs for processing the positional and density data from the microdensitometer have been completed. Also, a program package for simulating scanned aerial photographs in various orientations has been written. It will test the effects of the three-directional rotations on digital image matching procedures.

Development of a linear discriminate function (LDF) to automatically classify forest types on panchromatic prints was continued. While the LDF models performed well on the data used to estimate the coefficients of the model, performance dropped considerably when the model was applied to a new randomly selected data set. A new technique, called non-parametric density estimation, was tried in an attempt to overcome some of the deficiencies of the LDF. The non-parametric technique was no better than the LDF. It was found that our digitized panchromatic photography was insufficient to separate the forest classes defined. Recognition research will continue using the LDF

approach on small-scale color photography.

Preliminary estimates of timber volume and growth will be computed for the Stanislaus National Forest test area using a four-stage probability sampling design. A large-scale test of a five-stage forest inventory procedure using Apollo 9 and aerial photographs was conducted on 10 million acres in Louisiana, Mississippi, Arkansas and Georgia. A sampling error of only 13 percent was obtained on an estimate of 2.2 billion cubic feet of timber growing on 5 million acres in the Mississippi Valley. Additional work is being conducted to refine the estimating procedure for Georgia.

A prototype mapping system was developed after a preliminary system had been assembled and successfully tested, as reported in the previous annual progress report (Langley, et al., 1969). The main differences between the two systems is one of peripheral nature, stemming from the fact that the prototype system operates with actual scanned photographs, while the preliminary system was tested with simulated scanned photographs.

ACKNOWLEDGEMENTS

This research is being conducted under the Earth Resources Survey Program in Agriculture/Forestry under the sponsorship and financial assistance of the National Aeronautics and Space Administration, contract No. W12,996 ~~R-09-038-002.~~ The equipment used and salary of the principal investigator, as well as a portion of the salaries of several other professional employees, were contributed by the Forest Service.

Grateful acknowledgement is given the University of California, School of Forestry and Conservation, for their cooperation in providing doctoral candidates to assist in this study.

TABLE OF CONTENTS

Abstract i

Acknowledgements iii

Introduction 1

The Earth Resources Information System 2

Automatic Interpretation of Forest Types 7

The Prototype Automatic Mapping System 13

Literature Cited 32

THE DEVELOPMENT OF AN EARTH RESOURCES
INFORMATION SYSTEM USING AERIAL
PHOTOGRAPHS AND DIGITAL COMPUTERS

by

Philip G. Langley
Jan Van Roessel
David A. Sharpnack
Robert M. Russell

INTRODUCTION

One of the great opportunities in the exploration of earth resources from space is the development of a dynamic forest resource information system based on the analysis of imagery and/or data obtained from remote sensors. The system should be capable of supplying extensive up-to-date information to resource planners on a regional or national basis. In addition, it should be able to provide more intensive, in-place information to resource managers in selected local areas, such as national forests.

The conduct of an extensive forest inventory using space and aircraft photography, covering 10 million acres in Louisiana, Mississippi, Arkansas and Georgia, was described at the Second Annual Earth Resources Aircraft Program Review, NASA, MSC, Houston, Texas (Langley, et al., 1969). The sampling design used in that inventory is an extension of the design used in the more intensive inventory of the forest resources in the 100,000 acre Cosumnes Working Circle, Eldorado National Forest, being used as a test site for this research study. This typifies the kind of forest inventory, based on remote sensor data, that we intend to implement as an integral part of the wildland resource information system.

Even though it is not feasible to collect detailed ground data on every acre of land, it is feasible to have estimates of those data associated with the location of timber stands of localized areas. Such an area would be a national forest, a state forest, or a private holding. Information about the location of forest resources is as important to the local manager as information about the quantity and quality of those resources. Therefore, the resource information system being developed at the Pacific Southwest Forest and Range Experiment Station will accommodate detailed estimates concerning the resource base that are described by strings of coordinates defining their boundaries. Sample estimates are extended to individual parcels by means of statistical techniques. Boundary information will also be useful in keeping track of the location of sampling units in extensive surveys based on data from satellites or aircraft.

In last year's annual report, we briefly discussed various aspects of a forestry-oriented earth resources information system including (1) the nature of the information system -- its purpose and structure, (2) the data inputs to the system obtained from the interpretation of space and aerial photos, and maps by either manual or automatic methods, and (3) the interaction between the information system and multi-stage sample surveys using spacecraft and aircraft imagery and data collected on the ground.

This past year has been spent in further developing (1) the central portion of the resource information system itself -- the data handling programs, (2) techniques for automatically processing pictorial data by means of a photo scanner to provide data inputs to the information system, and (3) a multi-stage sampling design utilizing spacecraft and aircraft imagery for forest inventory. The remainder of this report describes the progress made during the year in each of the three areas mentioned above.

THE EARTH RESOURCES INFORMATION SYSTEM

Data Entry and Processing

Previous work involved (1) a definition of capabilities which the information system should have, (2) an identification of likely problem areas, particularly the question of the structure of the data base and the type of storage medium to be used, and (3) the kinds of equipment needed -- in short, a preliminary systems analysis. Our analysis of the overall structure of the system has proceeded to the point where detailed construction of the software has begun. This has consisted of obtaining equipment (a Bendix map digitizer), working out algorithms for processing the data and writing programs to test the algorithms and to test data entry procedures with particular reference to minimizing and detecting human errors.

Our systems analysis began with a refinement (Figure 1) of the previously produced system flow chart. It emphasized the division of the information system into two main functions: (1) the establishment and maintenance of the data base and (2) the processing of retrieval requests. The first function allows for coordinate data entry of points, lines and boundaries together with identification and for entry from punch cards of other detailed information. As the data are entered they are checked for consistency, refined if necessary (e.g., removing redundant information) and put into machine format. Digitized graphical information, such as the boundaries of sampling units or timber stands, is combined at this point with related punch card information. The finished data items are plotted on a digital plotter for the user to check for correctness. Further entries can be made to correct errors. The finished items are stored on disc or drum and also on magnetic tape. An index to the data base is also constructed and stored.

The retrieval function begins with the user formulating a request which is structured as a logical arrangement of relationships that must obtain in the items which the user wants retrieved. The computer searches the data base index to find any output items that satisfy the search request. Output is in

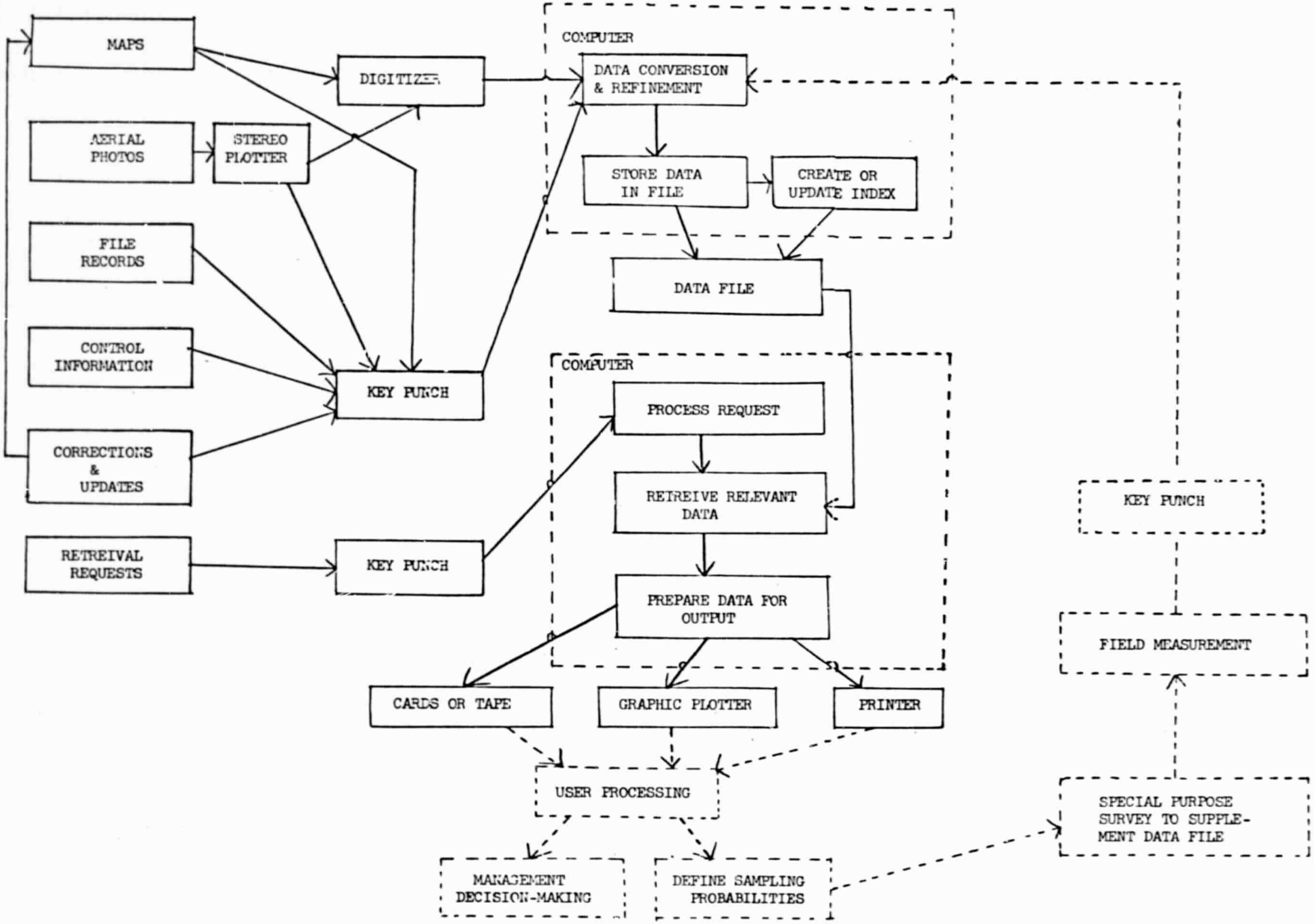

Figure 1. Wris Flow Chart

both printed and graphical form.

Underlying both functions is the question of the structure of the data base and the type of storage medium containing it. The data base is in three parts: (1) locational items (points, lines, boundaries together with descriptor labels); (2) an inverted index to it showing location of each descriptor, and (3) the topography function giving elevations at grid points in the area covered by the data base. Parts (1) and (2) are in the form of a multilist file with ring structure to provide efficient access.

For rapid retrieval it is essential that the data base be stored in a random-access medium such as disc or drum. It will also be stored on tape as a backup. Computer systems not allowing permanent disc or drum storage will have to copy the backup tape into the disc or drum before doing retrieval functions.

All programming is to be in ASA Standard Fortran and written to facilitate conversion between computers. This is essential to protect the programming investment.

Algorithms that have been devised concern the reduction of data entering from the digitizer in the data-base section of the information system, and the basic logical operations of the retrieval phase -- the two most critical areas of operation other than input and output.

The digitizer records lines and boundaries as a series of X-Y increments taken at .01 inch intervals. These data may originate from maps, space or aerial photos or other kinds of remote sensor data. There being more coordinate data than necessary by about a factor of 10, we developed an algorithm to thin out the unnecessary points. The number of points deleted varies inversely as the degree of curvature in the line. When a boundary is recorded, the operator cannot always finish at the exact starting point so we developed an algorithm which automatically closes the boundary, or signals an operator error if the discrepancy exceeds a predetermined amount. Another algorithm computes the area within a boundary.

Another critical retrieval process involves the determination of the intersection and union of two regions enclosed by boundaries.

In the course of developing algorithms we worked out an efficient internal storage scheme for a line or boundary. Maximum and minimum values of both X and Y are stored. In most cases, inspection of these extreme points suffices to show that a given pair of boundaries cannot intersect, or cannot have a union, thus short-cutting time consuming calculations. The scheme also accounts for "multi-lobe" boundaries -- regions composed of two or more disconnected sub-regions.

Testing data entry procedures received some attention due to the importance of having correct data in the data base. To provide a graphic means of checking and verification, we wrote a program which plots by means of a digital incremental plotter every point, line and boundary that was digitized. The operator can then compare this with the original. A common error is omission of items. The plotter output quickly shows up missing items.

The plotting program was used in debugging the previously mentioned algorithms because in many cases a visual check of the results is the quickest and best method to evaluate the effect of the algorithms.

We have identified some problem areas that will require close attention as we proceed with our work. The question of input-output efficiency is crucial if the final system is to be economical. The trouble is that the computer will spend much of its time doing input and output while searching the data base, yet modern computers are relatively slow in this area. Also, the input-output supervisory systems found on most computers are not very flexible. The only solution, short of acquiring very elaborate hardware, is in making maximum use of available equipment through good programming and systems analysis.

As we have indicated earlier, data entry is subject to human error. This will continue to receive much attention. The best solution with computer systems currently available seems to be to provide as much interaction as possible between computer and user, with frequent feed-back to the user for manual checking. This is a bit awkward without some kind of time sharing but a great deal can still be done using a batch system terminal available at the Pacific Southwest Forest and Range Experiment Station where the investigators are headquartered. Ultimately, of course, the algorithms in the resource information system should be re-programmed for a time-shared interactive computer system. This can come when a sufficiently economical system is developed for the kinds of processing and the size of the data file.

AUTOMATIC INTERPRETATION OF FOREST TYPES

Work Accomplished

Work on automating photo interpretation of forest types continued using the Challenge Experimental Forest as the study area. As reported in last year's annual report, a grid of cells .104 inches on a side superimposed on 9 x 9 inch aerial photos, comprises the basic data for this study. Each cell contains a 20 x 20 array of density measurements made on a lathe type helical scanner by the National Bureau of Standards. Eight density levels were recognized. By standard methods of photo interpretation, each cell was assigned to one of the eight forest types listed in Table 1.

Five new independent samples were drawn at random from the scanner data. Each sample contained 50 observations (cells) from each of 5 forest types. The forest types sampled were open conifer, conifer, conifer-hardwood, hardwood-conifer and open areas. These samples were used to test the behavior of the LDF

Table 1. Ground Cover Types for Challenge Experimental Forest

NUMBER	TYPE CODE	TYPE NAME	DESCRIPTION
1	OC	Open Conifer	Conifer forest with low density as in selection cuttings
2	C	Conifer	Mixed conifer with only occasional hardwood
3	CH	Conifer-Hardwood	Conifer with up to 50% hardwood
4	HC	Hardwood-Conifer	Hardwood with up to 50% conifer
5	H	Hardwood	Pure Hardwood
6	D	Developed	Town of Challenge and surrounding residential area
7	O	Open	Clear cut areas
8	M	Miscellaneous	Small areas not in first 7 types

and the non-parametric density estimation technique and to compare the two methods.* The same set of variables was used to obtain all of the results described here. There were the first, second and fourth moments, the first and second moment squared, position on the picture squared and sun angle. Each of the five samples was used as a training sample to classify the other four samples.

In addition to a lower error rate, the LDF provides more consistent results when different training samples are used. An indication of the kinds of error that were made is given by the error tally for the LDF (Table 3). The tally is similar for the density estimation method.

The results of the discrimination among all five forest types are not satisfactory. In looking for the reasons for this performance the distribution of each variable by type was plotted. A typical histogram (Figure 2) shows that the distributions for the first four forest types are very similar. In using these particular variables, we cannot expect much better results regardless of the technique used. The exception to this conclusion is the distribution of the fifth type -- open areas. It is distinctly different from the distribution of the other four forest types and we can expect that adequate discrimination can be obtained.

By examining the distribution of errors using the LDF model (Table 3) we can see another division of the ground cover into populations which will be useful. Table 3 shows that about 76% of the open areas and 85% of the open-conifer areas are identified correctly. Of the 3,000 observations belonging to the other three forest types, only 18% are identified as coming from either open-conifer or open type. Thus, it should be possible to separate the total

---

* The term "LDF" (Linear Discriminant Function) pertains to a multi-variate classification scheme which assumes that all variables have the normal distribution pattern, whereas the "non-parametric density estimation" is not based on this assumption. For further explanation see our September 30, 1969 Progress Report.

Table 2. Proportion of Correct Classification

Training Sample	LDF	Density Estimation
1	.424	.478
2	.426	.421
3	.426	.492
4	.434	.554
5	.425	.512
Mean	.427	.491

Table 3. LDF Error Tally.

		Predicted Type				
		OC	C	CH	HC	0
True* Type	OC	854	86	14	12	34
	C	171	438	76	238	77
	CH	163	199	201	389	48
	HC	58	165	129	615	33
	0	116	59	49	19	757

*Each row contains 1,000 test cases

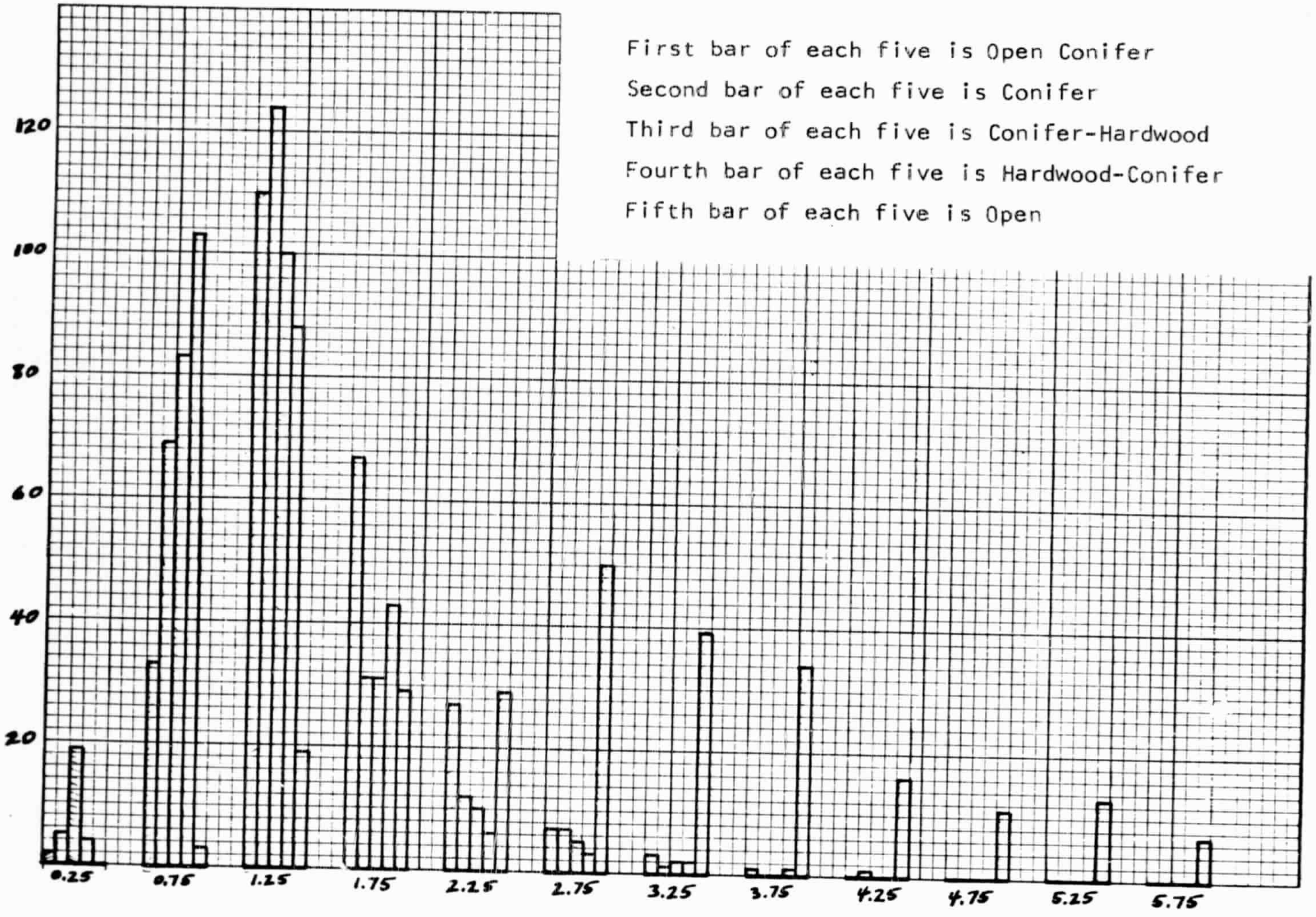
First bar of each five is Open Conifer
Second bar of each five is Conifer
Third bar of each five is Conifer-Hardwood
Fourth bar of each five is Hardwood-Conifer
Fifth bar of each five is Open

Figure 2. Distribution of M by types

forest area into categories by canopy density using this method.

By examining the error tallies from both discrimination techniques we can see why some of the other classification errors may have occurred. For example, the 116 open areas classified as open-conifer by the LDF model could arise from two possible sources. First, it is difficult in such a broad category to define a precise line between what is an open area and what is just a slightly wider spacing within a low density forest area. Second, the random placement of the cells on the open-conifer areas and the open areas may mean that a cell falls exactly on a small opening in an open conifer type or that it contains one tree in an otherwise large open area. This would tend to confuse any classification scheme. Another similar case appears in the tally for the density estimation technique for those cells known to be conifer-hardwood type. A cell known to be a conifer-hardwood cell is almost equally likely to be classified as a conifer-hardwood or hardwood-conifer. It is possible that this is a function of the cell size and of the clumpiness of the hardwoods within the conifers or the conifers within the hardwoods.

In comparing the results of the two methods (Table 2), we found that in almost every case the LDF performs better than the non-parametric density estimation technique. This, despite the fact that some of the variables, particularly the moments, are not normally distributed. When we look at the tally of errors we found that in all cases, except the classification of conifer-hardwood, the LDF yields significantly more correct classifications.

The LDF was found to have four advantages over the Density estimation technique:

1. the error rate was lower
2. the results are more consistent when different training sets are used
3. it is faster to classify a new point with the LDF and

4. less computer storage is required for the LDF.

Work in Progress

A new study has been started which will bring the goals of the automatic interpretation work closer to the needs of the multi-stage sampling designs. Randomly selected sample points on 1:110,000 scale RB-57 Ektachrome transparencies of the El Dorado Study Area, Mission 100, are being scanned on a PDS Series 1000 microdensitometer. The land types being sampled are those which should be useful in stratifying primary stage samples in a multi-stage sample design. These are forests by density and size, brush, grass, rock, water and roads. The study will be limited to work on the LDF model with the main effort devoted to finding useful variables for this type of classification problem.

THE PROTOTYPE AUTOMATIC MAPPING SYSTEM

One pair of scanned aerial photographs was used to test the prototype system, namely the photographs FS 2-44 and FS 2-43 of the Challenge Experimental Forest panchromatic photography of scale 1:10,000. (Obtained with K17 camera, 12" focal length; no calibration data were available.) These photographs were scanned by the National Bureau of Standards with a precision optical scanner described by Moore, Stark and Cahn (1964). The output of the photocell of the scanner was quantized into eight grey levels and recorded on magnetic tape. Each photograph was recorded in the form of 1728 scan lines, each consisting of 1728 spots. One grey value was associated with each spot. Thus, each photograph was represented by slightly less than three million grey values. The size of each spot was 0.132 mm, both in the x and y directions.

All processing was performed on a UNIVAC 1108 with an available core memory of 65,536 words. With this capacity, maximum areas of $16cm^2$ on both the left and right photographs can be stored in the memory core at one time. This amounts to 17,600 words for a total of 211,200 grey values, stored 12 to a word. The rest of the available memory is occupied by systems routines and the image matching program. Thus, the size of the available memory is the limitation for the maximum size of the stereo model that can be handled at one time. To facilitate the following discussion, the portion of the model handled in any one run will be referred to as a quadrangle, and the corresponding images such as the 16cm^2 portions of the scanned photographs used will be named the quadrangle images.

Whenever a visual representation of the scanned version of the photographs was necessary, a print-out was obtained in which each grey value was represented by a print character with an optical density related to the grey value. Examples of print-outs obtained from the scanned photographs 44 and 43 can be found in the 1968 Annual Progress Report (Langley and Sharpnack, 1968). A stereogram representing a small part of the stereoscopic model formed by the scanned photographs is presented in Figure 3.

The mapping system was first tested on a small 4cm^2 quadrangle situated in the middle of the stereomodel formed by photographs 44 and 43. Extensive tests were made on this area. They were evaluated mainly with the help of 16 control points whose positions were determined by means of analytic aerotriangulation.

After these tests, the feasibility of the overall approach was evaluated by mapping approximately half of the available stereomodel. This was accomplished by processing four 16cm^2 quadrangles, one at a time. For one of these areas an alternative hypsocline chart was made semi-manually, by measuring 121 elevations of points situated at the grid points of an 11 x 11 grid. These evaluations were converted to a hypsocline chart with the equally spaced data point method. This chart was compared with the automatically compiled one, to get a visual impression of the accuracy of the method. All phases of the mapping procedure were timed, so that the overall efficiency could be evaluated.

Before the various tests are described in more detail, a more thorough description of the prototype mapping system is deemed appropriate.

The Prototype Mapping System

The prototype mapping system differs from the preliminary measurements, which, in the present case, were made on the photographic prints with a coordinatograph. These measurements are converted to model coordinates with the strip-triangulation program. Because the resulting points are not equally spaced, a second degree surface is fitted through them with the unequally spaced data point method. Equally spaced output derived from the fitted surface is then input to the program for equally spaced data points to obtain the surface coefficients for the predictive phase. With the preliminary mapping system, the original model used to generate the simulated photographs was directly available for prediction.

After the terrain model is known, and if the fitting process has been confined to a rectangular area in the model space, the points forming the corners of this area are projected onto the left and right plates with the help of the data derived from the aerotriangulation. The plate coordinates of these projected corner points are then converted to scanner coordinates (line and spot number), and subsequently to the appropriate tape addresses, for retrieval of the quadrangle images to be used for the matching process. These images are stored on a fast drum, ready for use by the image matching program.

The image matching program of the prototype mapping system has routines to accomplish the prediction of conjugate points and the following image matching that are identical with routines of the preliminary mapping system. Some peripheral differences are present. The number of grey levels used is 8 instead of 16. A number of rotations and translations has been incorporated to refer the match data, originally in the coordinate system of the search area to the coordinate system of the quadrangle image and from this system to the scanner coordinate system. The number of outliers is always three, providing adequate redundancy for the quality control procedure.

The quality control procedure is a major addition to the mapping system. The Y coordinate of a point in model space can be computed in two ways, each yielding a slightly different coordinate. The discrepancy can be used to screen out unwanted points. Although the positions of the conjugate points can be predicted to the very scan line, the right search area is purposely not restricted to one line. Thus, if a false match occurs, it is likely to happen elsewhere in the search area, where the resulting model point will have excessive Y parallax. All points with such parallax exceeding a certain limit are rejected. The mean and standard deviations of the remaining points are computed, and only points within one standard deviation of the mean are retained for surface fitting.

Finally, the coordinates of the matched points are computed in the model space, with scale identical to that of the photographs, instead of using the local coordinate system. The results of the surface fitting program have to be subjected to a block adjustment program to be converted to the local coordinate system.

Evaluation of the Numerical Accuracy of the Prototype System

In order to make a fairly extensive investigation in the form of different experimental conditions, a small 4cm^2 quadrangle was selected in the middle of the stereomodel of the photographs 44 and 43. In the stereogram of Figure 3 the area is represented by the outlined square situated at the middle of the right side of the stereogram. The area is mostly open with adequate contrast but also contains tall vegetation in the upper left and lower right corners, where some tree heights of 25 meters could be measured. A stereogram of the scanned quadrangle images is presented in Figure 4.

A control point net of 16 points, determined by analytic aerotriangulation, was superimposed on the quadrangle. In this manner the accuracy of the automatic system could be evaluated through a comparison with measurements obtained with an entirely different method.

Before the experiment is described in detail, the theoretically best obtainable accuracy should be commented on. In the case in which there are only broad parallax trends, and in which no high frequency parallax components caused confusion between vegetation and man-made objects, matching can be accomplished to the nearest spot, and the best possible accuracy can be computed accordingly. For the prototype system, in combination with the photographs used, a different kind of reasoning has to be employed.

First, the effect of the vegetation has to be considered. The perfect match, to the nearest spot, will occur perhaps somewhere within the 8 x 8 frames used for image matching. The upper left hand corner of these frames is presently used to compute the position of the model points. Because of relief variation within the frame, and due to a differential rotation between the photographs, there will be a discrepancy (dx,dy) between the corners of the two frames. One can calculate that for a spot size of 0.132 mm the elevation discrepancy within the 8 x 8 frame would have to amount to 4.56 meters on the ground, to give rise to a discrepancy dx or dy equal to the spot size. This discrepancy could easily occur through the vegetation present. It is extremely difficult to give a precise estimate of the standard deviations of the discrepancies between the corresponding 8 x 8 frames, other than that they have to be multiples of the spot size. For the present experiments, the standard deviation of the Y parallax was equal to one spot size, or slightly less.

Secondly, because of the quality control procedure, only a small part

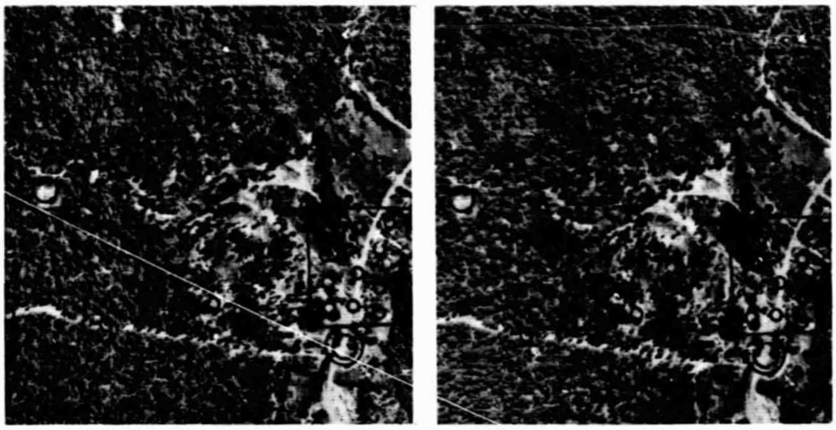

Figure 3. Stereogram of half stereomodel formed by photographs 44 and 43

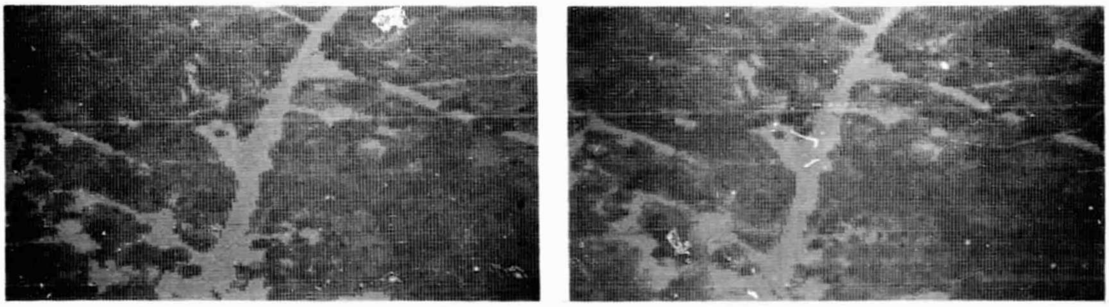

Figure 4. Stereogram formed by printout of picture tapes. The area corresponds to the enclosed section of the above stereogram.

of the Y parallax and X discrepancy distribution is being propagated in the surface fitting process. At present, only those points with Y parallaxes that are within 1 standard deviation of the mean Y parallax are being used in the surface fitting process. Assuming that the Y parallaxes and the corresponding X discrepancy distributions are normal distributions, the normal distributions truncated at one standard deviation will have a new standard deviation of 0.626 of the old standard deviation. Therefore, when the standard deviation of the Y parallax distribution is one spot size, corresponding to an elevation difference of 4.56 meters on the ground, the quality control procedure will reduce the standard elevation error to 2.85 meters. Finally, it should be kept in mind that the accuracy of the fitted surface points is not equal to the Root Mean Squared Error (RMSE) that can be computed from the deviations of the data points and the fitted elevations.

Thus, the theoretical best obtainable accuracy cannot easily be evaluated without elaborate error propagation considerations, and the best cut off limit for the Y parallax of points to be used in the surface fitting process is not easily established. Nevertheless, the one standard deviation limit seems to be a reasonable one.

Experimental test runs were made to test the following hypothesis:

a. An increased size of the left search area results in improved accuracy.

b. An increased size of the right search area results in improved accuracy.

c. The use of the second computation level provides more accurate results than can be obtained with the first level.

Hypothesis A was entertained with the idea that a larger search area on the left photographs provides a better choice of outlying images, and therefore better results. Hypothesis B was proposed to determine the influence of an increase of the right search area, which could either increase or decrease the overall accuracy, depending on whether the right search area was too small, adequate, or too large. Hypothesis C was to be tested to confirm the positive results obtained with the preliminary mapping system.

The experiment was performed in the form of a balanced half-replicate of the 2^3 factorial outlay. The experimental conditions (1), a, b, c, and abc correspond to test runs under the following conditions pertaining to the above hypothesis:

	Left search area size (spots)	Right search area size (spots)	Computation level
(1)	8 x 8	12 x 12	1
a	12 x 12	12 x 12	1
b	8 x 8	16 x 16	1
c	8 x 8	12 x 12	2
abc	12 x 12	16 x 16	2

For all runs the matching grid was an 11 x 11 grid of 121 points. Three outliers were selected in the left search area, so that the total number of points matched was 363. Only those points witnin the Y parallax standard deviation from the mean were retained for surface fitting. All surfaces were fitted with a maximum polynomial power of 5. The accuracy was evaluated by comparing the elevations of the surfaces with those of the control points. Root mean square error (RMSE) values were computed. The test results are displayed in Table 4.

The RMSE values of the first three columns of Table 4 reflect the basic accuracy of the present automatic mapping system, as well as could be determined under the circumstances. They were originally computed in the model space at a scale equivalent to the original photo scale and then multiplied with the denominator of the scale fraction to arrive at the values on the ground.

Table 4. Results of Experiment with 4 cm^2 Quadrangle

Experimental Condition	RMSE about surface	RMSE from control (meters)	RMSE from control (corrected)	Mean Y parallax (mm)	Stdv Y parallax (mm)	% points n-m stdv from mean, where n-m is:			
						0-1	1-2	2-3	3+
							%		
(1)	4.74	5.90	4.76^2	-0.058	0.128	63.7	24.0	5.5	6.8
a	3.60	5.53	4.39^1	-0.055	0.114	64.5	21.3	5.2	9.0
b	6.31	5.69	4.95^1	-0.060	0.128	59.3	21.3	5.7	13.7
c	2.63	4.26	4.26^0	-0.077	0.104	71.0	21.9	1.9	5.2
abc	2.20	3.42	3.42^0	-0.081	0.099	69.7	23.8	2.7	3.8

The second column of Table 4 gives the RMSE values about the fitted surface, that is, the RMSE computed from the discrepancies of the fitted elevations and the elevations of the matched points. The third column presents the RMSE values obtained with the independent set of control points. The values of the fourth column were also computed with these control points, but they have been corrected for large discrepancies at the edge of the quadrangle. These occur because at times the configuration of the matched points leaves parts of the very edges of the model uncontrolled, due to its unequally spaced nature. The superscript indicates the number of points that were removed; no corrections were necessary for runs at the second computation level.

It should be kept in mind that the elevations of the control points are by no means without error. For tests conducted with photography of the same scale, the RMSE of the control points (computed with the true elevations) amounted to 2.88 m, equal to the RMSE that can be expected for the matched points after application of the quality control procedure. The values of the fourth column therefore do not reflect the true RMSE that could have been computed if the true elevations of the control points had been known.

In the following two columns of Table 4 the mean Y parallax and the standard deviation of the Y parallaxes are listed. The mean Y parallax is close to half the spot size for most runs, a fact that can be readily explained from the discrete nature of the scan lines, which in general do not coincide with the lines of equal Y parallax. The standard deviation is approximately one spot size; it is slightly less for the runs at the second computation level. This could be expected in view of the earlier discussion on the best obtainable accuracy.

In the remaining columns of Table 4 the percentages of points that are 0-1, 1-2, 2-3, and 3+ standard deviations removed from the mean Y parallax are presented. The corresponding percentages for a normal distribution would be:

68.27, 27.18, 0.034 and 0.002, respectively. It can be concluded that the percentages agree quite closely for the 0-1 and 1-2 standard deviation portions of the normal density curve but not for the tail areas, where it seems that the observations belong to a distribution with a much larger standard deviation. This appears logical, since most of the observations in the tails are blunders, with Y parallaxes of an entirely different nature. Thus, it seems fair to conclude that the distribution of Y parallaxes is probably a scale contaminated compound normal distribution, with much heavier tails than if they conformed to a pure normal distribution.

Three responses for the balanced half replicate 2^3 experiment were used: (1) the RMSE about the fitted surface (the values of the second column of Table 4); (2) the corrected RMSE values derived with the independent control points (the fourth column of Table 4); (3) the 0-1 and 3+ columns of the Y parallax frequency histograms. These last responses were selected because they are representative of the number of high quality matched points and the number of points that are blunders.

For the four types of response the M (mean), A (left frame size), B (right frame size), and C (computation level) effects were computed. Also, the sum of the interactions AB, AC and BC could be computed. The results are presented in Table 5. Although no error estimate is available for the experiment, it is still possible to draw conclusions with regard to the proposed hypotheses. It can be assumed that it is fair to accept a hypothesis when the corresponding effect exhibits the appropriate signs for all four responses. Thus, if hypothesis A were true, the first two entries for the effect A would be negative, since the RMSE would decrease; on the other hand, the third entry would have to show an increase (more high quality points), and the last entry should be

Table 5. Effects for Experiment with 4 cm^2 Quadrangle

Effects	Responses used			
	RMSE about surface	RMSE from control corrected	% points 0-1 stdv from mean	% points 3+ stdv from mean
M	3.896	4.356	65.640	7.70
A	-0.731	-0.309	0.831	-0.87
B	0.624	-0.029	-1.768	2.41
C	-1.216	-0.374	4.081	-2.77
AB+AC+BC	-0.215	-0.065	0.575	-2.63

negative, as fewer blunders would be made. It can be seen in Table 5 that this is indeed the case, so that hypothesis A cannot be rejected. The signs of the values for the B effects are just the reverse of those of the A effects, except for the value of the second response, however, this value is close to zero, so that it can be concluded that hypothesis B cannot be accepted. Apparently, the 12 x 12 search area on the right photograph is of adequate size. A size increase merely reduces the probability that the left 8 x 8 frame will have a unique corresponding frame on the right photograph, so that more blunders can be made. This is evident from the relatively high B effect in the fourth column. As for hypothesis C, the results in Table 5 indicate conclusively that the use of the second computation level increases the accuracy considerably, thus confirming the results of the previous experiments. It is especially noticeable in the gain of high accuracy points and a decrease in blunders, as can be seen in the third and fourth columns. Finally, among the sums of the two-factor interactions, the fourth sum is of considerable relative magnitude. This may be caused by the interaction, BC, which results from a lessening of the increase in blunders due to a larger right search area, because of the higher computation level. At the second level more information of the 8 x 8 frames is utilized.

Evaluation of the Prototype System by Mapping Half a Stereomodel

To make a realistic evaluation of the capabilities of the prototype mapping system, half of the stereomodel formed by the photographs 44 and 43 was mapped. This was accomplished by dividing the area into four quadrangles, each of which was treated separately. The size of each of the quadrangles was 16 cm^2, which is the size of the maximum area that can be handled by the image matching program at one time. The total area mapped is shown in the stereogram of Figure 3, which can be divided into four sections corresponding to the four quadrangles. The vegetation present in each quadrangle can be characterized in order of decreasing overall density as follows:

Quadrangle	Vegetation
I. (upper left)	Conifer - Hardwood; Conifer
II. (lower left)	Conifer
III. (upper right)	Conifer; Conifer - Hardwood; Open
IV. (lower right)	Open; Conifer

For each quadrangle, nine control points were marked on the photographs, for which the model coordinates were computed with the strip-triangulation program. Through each set of nine model points a quadratic surface was fitted with the unequally spaced data point technique. The quadratic terrain models were used as starting models for the prediction process.

A run of the image matching program was made for each of the quadrangles. The matching grid was a 15 x 15 grid in each case; three outlying points were used per grid point, so that 675 points were matched for each quadrangle. Considering 2 mm margins, this amounts to approximately 1 point per 1.4 mm^2. The sizes of the search areas used were 8 x 8 and 16 x 16. The increase of the right search area with respect to the 12 x 12 one used for the 4 cm^2 quadrangle was justified on account of the increased variation in the terrain relief.

The results of the runs of the image matching program are presented in Table 6.

The entries of Table 6 correspond to those of Table 4. However, insufficient independent control points were available for the computation of a RMSE from control points.

Some remarkable differences can be observed between the values of Table 4 and Table 6 which are due to the fact that the 4 cm^2 quadrangle was primarily open with scattered tall trees, while the 16 cm^2 quadrangles are heavily vegetated. In general, the number of high quality points appeared to be about 20% less, while the number of blunders showed an increase of approximately 20%.

Table 6 Results of Image Matching Runs for Half a Stereomodel

Quad.	RMSE about surface (meters)	Mean Y par.	Stdv Y par.	% points n-m stdv from mean, where n-m is:			
				0-1	1-2	2-3	3+
I	15.46	-0.045	0.162	37.8	17.4	11.2	33.6
I*	12.03	-0.074	0.135	46.6	14.4	6.5	32.6
II	11.80	-0.138	0.138	41.2	20.3	9.8	28.7
III	11.80	-0.053	0.158	47.6	18.8	9.8	23.8
IV	7.94	-0.167	0.140	54.9	15.7	9.2	20.1

* This run was done at the second comp. level

The percentages for the points that were 1-2 and 2-3 Y-parallax standard deviations from the mean remained of the same magnitude.

With respect to all the criteria of Table 6, the quadrangles can be ranked IV, III, II, I, according to the quality of the matching runs. This ranking corresponds exactly to the one relating to the density of the vegetation presented earlier. Quadrangle IV, with a considerable amount of open developed area, including the town of Challenge, gave the best results. On the other hand, quadrangle I, with a dense conifer-hardwood vegetation, was judged to provide insufficient points of high quality at the first computation level, so that the run for this quadrangle was repeated at the second computation level. This resulted in a considerable gain of high quality points (23%).

Also, one can see from Table 6 that in the case of quadrangles II and IV the mean Y parallax seemed to be biased. However, this bias could not simply be eliminated by shifting the right picture up or down over the appropriate distance. The standard deviation of the Y parallax was approximately equal to the spot size in all cases.

The coordinates of the high quality points were written on magnetic tape and then served as input to the unequally spaced data point surface fitting procedure. All four surfaces were fitted with hybrid polynomials with a maximum power of seven. Hypsocline charts were derived from the fitted surfaces. The assembled hypsocline map is shown in Figure 5. The hypsocline bands are 4-meter bands. The area in the form of a cross could not be mapped with the present method, because the edges of the quadrangles have to be avoided in order not to get the edge effects. However, this problem can be circumvented by providing the proper overlap between the quadrangles.

To obtain a visual impression of the accuracy of the hypsocline map, the lower right hand quadrangle was compared with an independent hypsocline map derived from 121 elevation measurements made on the Zeiss Stereotope in

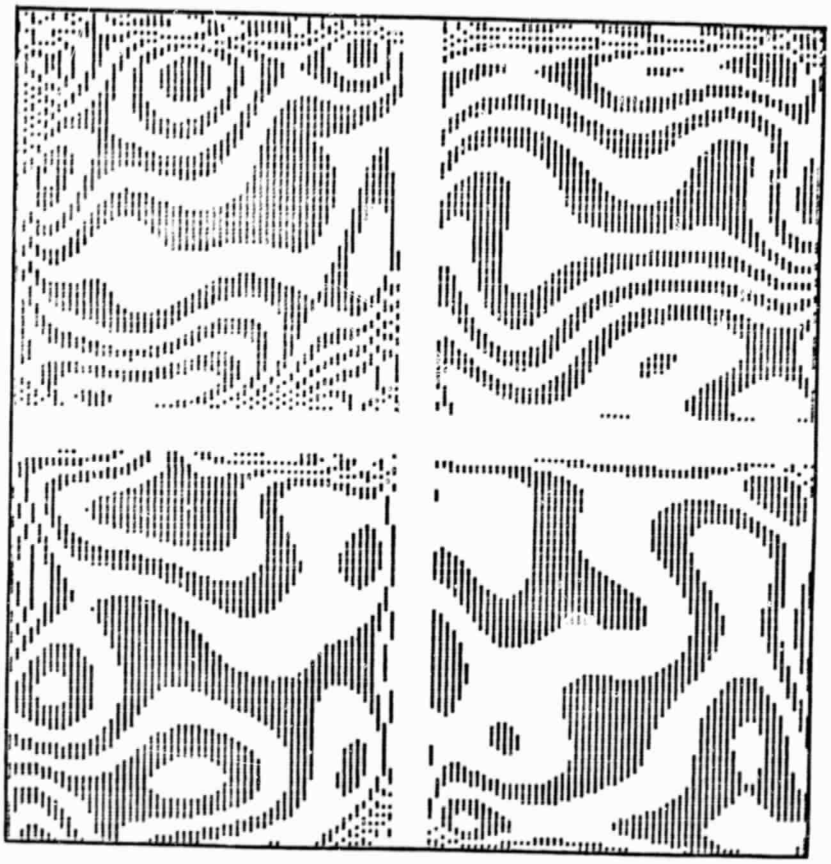

Figure 5. Assembled hypsocline map, half stereomodel, photographs 44-43.

the part of the 44-43 model corresponding to the fourth quadrangle. The elevations were measured at the points of an 11 x 11 grid situated in the pantograph plane of the Stereotope. A ninth power surface was fitted through the equally spaced point method; all elevations were measured on the ground surface as well as could be estimated. The hypsocline chart corresponding to the fitted surface is shown in Figure 6. There is a small scale difference between the two comparable hypsocline charts due to the fact that the margins could not be mapped with the automatic compilation process. Otherwise, identical hypsocline bands can be clearly identified, and in most cases the discrepancy is not larger than one band, comparable with the magnitude of the RMSE computed from the control points for 4 cm^2 quadrangle (see Table 4).

A further check of the validity of the hypsocline map can be obtained by visually comparing the map with the stereogram of Figure 3.

Efficiency of the Prototype Mapping System

At present the prototype mapping system is rather segmented. This is a direct result of the research-oriented nature of the program, where the possibility has to exist to subject every stage in the mapping process to close scrutiny. However, it is possible to consolidate several of the peripheral programs of the mapping system. It is expected that this will result in considerable savings of computation time, and it is estimated that the time for miscellaneous peripheral processing can be reduced to less than half of the present estimate.

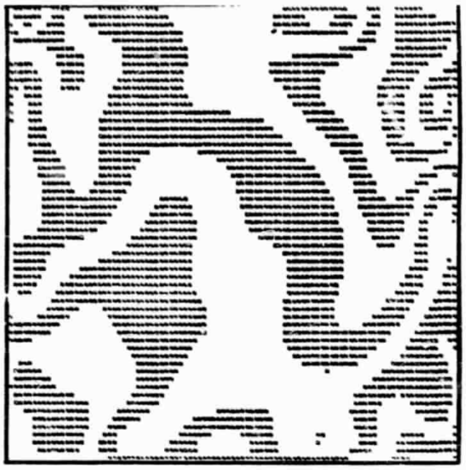

Figure 6. Hypsocline chart of quadrangle IV made from Stereotope elevation measurements.

LITERATURE CITED

Langley, P. G., R. C. Aldrich and R. C. Heller. 1969. Multi-stage sampling of forest resources by using space photography -- an Apollo 9 case study. Proceedings Second Annual Aircraft Program Review, NASA MSC, Houston, Texas.

Langley, P. G., D. A. Sharpnack. 1968. The development of an earth resources information system using aerial photographs and digital computers. Annual Progress Report, NASA Contract No. R-09-038-002, 30 September 1968, Forestry Remote Sensing Laboratory, Berkeley, California. 26 pp.

Langley, P. G., D. A. Sharpnack, R. M. Russell, and J. Van Roessel. 1969. The development of an earth resources information system using aerial photographs and digital computers. Annual Progress Report, NASA Contract No. R-09-038-002, 30 September, 1969, Forestry Remote Sensing Laboratory, Berkeley, California. 43 pp.